

A review on the pumping behavior of modern concrete

Li, Huajian; Sun, Deyi; Wang, Zhen; Huang, Fali; Yi, Zhonglai; Yang, Zhengxian; Zhang, Yong

DOI

[10.3151/jact.18.352](https://doi.org/10.3151/jact.18.352)

Publication date

2020

Document Version

Accepted author manuscript

Published in

Journal of Advanced Concrete Technology

Citation (APA)

Li, H., Sun, D., Wang, Z., Huang, F., Yi, Z., Yang, Z., & Zhang, Y. (2020). A review on the pumping behavior of modern concrete. *Journal of Advanced Concrete Technology*, 18(7), 352-363.
<https://doi.org/10.3151/jact.18.352>

Important note

To cite this publication, please use the final published version (if applicable).
Please check the document version above.

Copyright

Other than for strictly personal use, it is not permitted to download, forward or distribute the text or part of it, without the consent of the author(s) and/or copyright holder(s), unless the work is under an open content license such as Creative Commons.

Takedown policy

Please contact us and provide details if you believe this document breaches copyrights.
We will remove access to the work immediately and investigate your claim.

A review on the pumping behavior of modern concrete

Huajian Li ^{1,2}, Deyi Sun ^{1,2}, Zhen Wang ^{1,2}, Fali Huang ^{1,2}, Zhonglai Yi ^{1,2}, Zhengxian Yang ³, Yong Zhang ^{3,4,*}

¹ PhD, Railway Engineering Research Institute, China Academy of Railway Sciences Corporation Limited, No.2 Daliushu Road, Beijing 100081, China.

² PhD, State Key Laboratory of High Speed Railway Track Technology, No.2 Daliushu Road, Beijing 100081, China.

³ Professor, College of Civil Engineering, Fuzhou University, Fuzhou 350116, China.

⁴ PhD, Microlab, Section of Materials and Environment, Department of 3MD, Faculty of Civil Engineering and Geosciences, Delft University of Technology, 2628 CN Delft, The Netherlands. * Corresponding author, Email: y.zhang@fzu.edu.cn (Y.Z.)

Abstract: Pumping is the most common technique used to transport fresh concrete in construction sites. The large-scale use of concrete all over the world makes the pumping increasingly important. A wide variety of additives and admixtures are incorporated into modern concrete in order for sustainable development. The performance of modern concrete is rather complex and its pumping behavior differs significantly from that of conventional concrete, especially in the fresh stage. This paper presents a comprehensive overview on the state of the art of concrete pumping. The models and methods used for characterizing the concrete pumpability and lubrication layer are described. The factors influencing the pumping behavior are discussed. A couple of ultra-high pumping engineering of concrete conducted in China are introduced.

Keywords: modern concrete; pumpability; lubrication layer; model; review

1. Introduction

A broad range of construction techniques of concrete pumping has been developed globally. The pumping enables horizontal and vertical transportation of concrete at one time, which is labor-saving and cost-effective. In the cases where construction sites are narrow and obstacles are present, advanced pumping technique of concrete is of particularly interest (Jiang et al. 2017; Zhao 1985).

Significant progress has been achieved on the pumping behavior of conventional vibrated concrete (CVC) over the past decades, especially in the field of prediction of the pumping pressure, influencing factors of pumpability and rheological properties, and the friction performance of the lubrication layer (Kaplan 2001, Secieru 2018b). In order to sufficiently utilize various byproducts and wastes and improve the construction performance of concrete, different kinds of additives and admixtures are nowadays incorporated into modern concrete, e.g. self-compacting concrete (SCC) and high-flowability concrete (HFC). The properties of modern concrete are highly sensitive to the raw materials, temperature, age and operation methods, resulting in the pumping behavior of modern concrete to be quite different from that of CVC, particularly in the fresh stage. Unfortunately, the knowledge regarding the pumping behavior of modern concrete is far from sufficient up to date.

This paper presents recent advances on concrete pumping behavior, including the steady flow state, the pumping models, the test methods and the influencing factors. Previous experimental results related to these aspects are provided. The pumping behavior and associated problems facing the engineers are discussed. A few typical cases of the ultra-high pumping engineering conducted in China are introduced eventually.

48 **2. Steady flow state of concrete in pump pipe**

49 Fresh concrete is a kind of heterogeneous composite mixture with non-Newtonian fluid
 50 characteristics (Jiang et al. 2017). Pumped concrete is often considered as Bingham fluid
 51 sliding along the pump pipe under pressure, as shown in Fig. 1. The rheological properties of
 52 Bingham fluid can be described with Eqs. (1) and (2). Eqs. (3) and (4) can be deduced directly
 53 from Eqs. (1) and (2). From the boundary conditions $r = R$ and $v = 0$, Eq. (5) is obtained. The
 54 velocity distribution of the Bingham fluid during the pumping process can be illustrated in
 55 Fig. 2 (Zhao 1985).

$$\tau = \Delta P \frac{r}{2l} \quad (1)$$

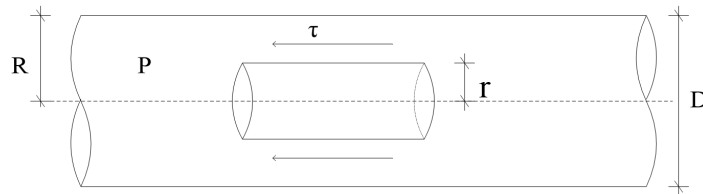
$$\tau = \tau_0 + \eta \frac{dv}{dr} \quad (2)$$

$$\frac{dv}{dr} = \frac{1}{\eta} \left(\frac{\Delta P r}{2l} - \tau_0 \right) \quad (3)$$

$$\int \frac{dv}{dr} dr = \frac{\Delta p}{2\eta l} \int r dr - \frac{\tau_0}{\eta} \int dr \quad (4)$$

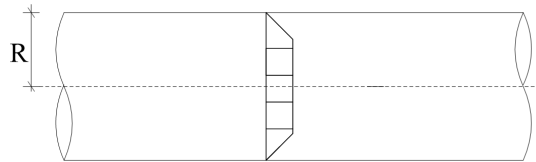
$$v = \frac{1}{\eta} \left[\frac{\Delta P}{4l} (R^2 - r^2) - \tau_0 (R - r) \right] \quad (5)$$

56 where r [m] is the distance from the axis of the pump pipe, τ [Pa] is the shear stress of fresh
 57 concrete when the distance from the axis of the pump pipe is r , ΔP [Pa] is the pressure
 58 difference of fresh concrete in the pump pipe, l [m] is the length of fresh concrete in straight
 59 pipe section, τ_0 [Pa] is the yield stress of fresh concrete, η [Pa·s] is the viscosity coefficient
 60 of fresh concrete, v [m/s] is the velocity of fresh concrete.



61
62

Figure 1. Bingham fluid sliding Model.

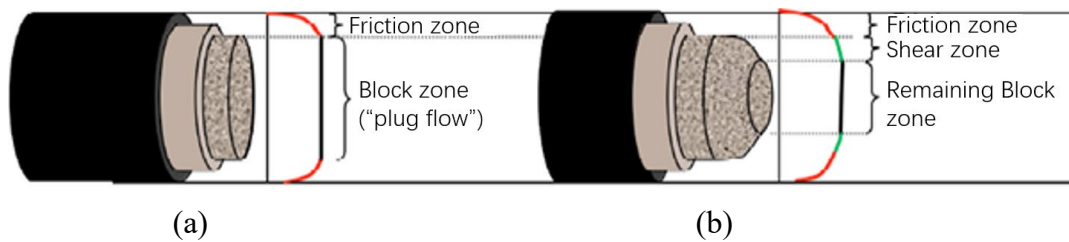


63
64

Figure 2. Velocity distribution of sliding Bingham fluid (Zhao 1985).

65 Kaplan (2001) stated that when sliding at low speed, the pumped concrete could be
 66 regarded as friction flow, also known as plug flow. The middle part of the plug flow,
 67 cylindrical in shape, is called block zone. According to Yan and Li (2018), the shear stress at
 68 each point of the cross section of the pump pipe is linearly distributed along the radius, and
 69 the shear stress is zero in the axis of the pump pipe. The maximum shear stress is near the
 70 inner wall of the pump pipe. The shear stress near the axis of the pump is less than the yield
 71 stress of the fresh concrete. This part of concrete will not produce relative slippage during
 72 the pumping process, thus forming the block zone. A friction layer known as lubrication layer

73 will be formed between the block zone and the pipe wall, as illustrated in Fig. 3 (a). During
 74 the pumping process, the formation of the lubrication layer can greatly promote the pumping
 75 process of the fresh concrete. When the flow rate of concrete mixture is larger, the pumping
 76 pressure is higher. Then the shear stress near the inner wall of the pump pipe may exceed the
 77 yield stress of the fresh concrete. In addition to the formation of lubrication layer and block
 78 zone, the fresh concrete will also form a shear zone between block zone and lubrication layer.
 79 This kind of flow state is known as friction flow and viscous flow, as illustrated in Fig. 3 (b).
 80 It is usual that CVC only has block zone and lubrication layer during the pumping process
 81 because of the high yield stress. SCC and HFC have high workability, resulting in their low
 82 yield stress. Besides the block zone and the lubrication layer, the shear zone can be formed
 83 during the pumping process of SCC and HFC.



84
 85
 86 **Figure 3.** Sliding model for the flow of fresh concrete in pipe (Kaplan 2001).

87 **3. Lubrication layer**

88 The concrete pumped in the pipe comprises two parts: bulk concrete and lubrication
 89 layer. The pipe flow of the pumped concrete is predominated by the lubrication layer. The
 90 relatively thin lubrication layer has a lower viscosity than the bulk concrete (Choi et al. 2013).
 91 Morinaga (1973) and Secrieru et al. (2018b) stated that concrete cannot be pumped without
 92 formation of the lubrication layer formed at the interface between the concrete and the wall
 93 of the pipe. The lubrication layer with appropriate thickness and stable state can reduce the
 94 effect of friction and make the concrete mixture have a better pumpability. In this respect an
 95 experimental investigation, as well as numerical verification, was carried out by Secrieru and
 96 Mechtcherine (2020).

97 **3.1. Formation of lubrication layer**

98 The hydraulic pressure gradient created during pumping facilitates the formation of
 99 lubrication layer (Secrieru et al. 2018a). The lubrication layer is a mortar-like layer formed
 100 on the pipe wall during the pumping process. The pumping resistance is in essence
 101 determined by the friction between the pipe and the lubrication layer (Kwon et al. 2013; Jo
 102 et al. 2012). The friction at the pipe-concrete interface occurs when fresh concrete flows (Ngo
 103 et al. 2010a, 2010b). The pumping can be operated only when the pump pressure is larger
 104 than the friction (Eda 1957; Browne et al. 1977; Le et al. 2015). During the pumping process,
 105 the concrete mix is filled in the pipe and pushed forward by the high pressure. Rossig et al.
 106 (1974) pumped colored concrete and observed a paste rich zone at the vicinity of the pipe
 107 wall. Jacobsen et al. (2009) prepared colorful concrete for pumping experiment and also
 108 observed an enriched mortar area near the wall. A redistribution of the particles takes place
 109 in the pipe under the shear action during pumping. In the process of concrete pumping,
 110 migration of the sands (fine particles) is ignorable as compared to migration of the gravel
 111 (coarse particles). Feys et al. (2015) stated that the lubrication layer is formed because of the
 112 coarse aggregate migrating to the pipe center (low shear zone) and leaving more micro mortar
 113 in the boundary region. The lubrication layer can therefore be considered as the constitutive
 114 mortar of the pumped concrete (Choi et al. 2013).

115 Lubrication layer is also termed boundary layer. Its capability to reduce friction plays an
116 indispensable role in the pumping process. Shearing takes place in the lubrication layer owing
117 to its lower plastic viscosity and yield stress relative to the bulk concrete. Based on the torque
118 and the angular velocity of the rotary cylinder, the plastic viscosity μ and the yield stress τ
119 of the lubrication layer can be determined as follows:

$$\tau_s = \frac{\Gamma_0}{2\pi h R^2} \quad (6)$$

$$\mu_s = \frac{k}{4\pi h} \left(\frac{1}{R_c^2} - \frac{1}{R_s^2} \right) \quad (7)$$

120 where Γ_0 is the initial torque to start the shear flow, h stands for the difference of the two
121 filling heights, k is a parameter by fitting the linearity between the angular velocity and the
122 torque, R_c refers to the radius of the rotary cylinder, R_s represents the distance from the end
123 of the lubrication layer to the center of the rotary cylinder.

124 In many cases the obtained rheology properties of concrete fluid are not consistent with
125 those predicted from the Bingham fluid or Herschel Buckley fluid theory. The main reason
126 can be ascribed to the ignorance of the properties of the lubrication layer (Kaplan et al. 2005b;
127 Feys et al. 2009). Most of the existing studies about lubrication layer are based on the CVC
128 while the research on modern concrete such as SCC and HFC is quite inadequate. The
129 quantitative relationship between lubrication layer parameters and concrete composition
130 remains a pending issue. To what extent can the rheological properties of concrete affect the
131 properties of lubrication layer requires further research.

132 3.2. Parameters of lubrication layer

133 (1) Composition

134 Complete description and detailed characterization of the lubrication layer are not easy.
135 The results reported in the literature are far from sufficient. However, significant progress
136 has been made in the composition of lubrication layer. As noted by Ngo et al. (2010a, 2010b),
137 the lubrication layer is normally composed of water, cementitious materials and fine sand.
138 The diameter of the fine sand is smaller than 0.25 mm. The content of water and cement is
139 basically consistent with that in the concrete, but the volume of fine sand in the lubrication
140 layer is higher.

141 (2) Thickness

142 Feys et al. (2009) stated that the rheological properties and the thickness of the
143 lubrication layer depended mainly on the mix proportion of the concrete under study. Choi
144 et al. (2013) reported a 2 mm thick of lubrication layer as measured by using ultrasonic
145 velocity profiler in the full-scale pumping circuits. Kaplan et al. (2005b) found the lubrication
146 layer has a thickness of approximately 1~5 mm. Ngo et al. (2010b) stated that the thickness
147 of lubrication layer for different concrete mixtures varied between 1~9 mm, and it was
148 increased with the increase in water-cement ratio, superplasticizer content and the volume of
149 cement paste but was decreased with the increase of the volume fraction of fine sand. From
150 the viewpoint of rheology, it can reduce the apparent plastic viscosity and increase the
151 thickness of the lubrication layer in a desirable range by reducing the content of fine sand,
152 increasing water-cement ratio and increasing superplasticizer content. Choi et al. (2013)
153 carried out further research on the lubrication layer through ultrasonic velocity profiler. They
154 found that the thickness of lubrication layer, which was 2 mm roughly, was not influenced
155 by the flow rate but mainly by the diameter of pipeline and volume of sand and gravel in the
156 concrete mixture. In previous reports the thickness of the lubrication layer was in most cases
157 determined directly from the velocity profile. Limitations still exist in precisely acquiring the

158 pure profile of the pumped concrete. In addition, there is a high need to consider carefully
 159 the lubrication layer thickness and associated rheological properties.

160 (3) Rheological parameters

161 Feys et al. (2014) suggested that the viscous constant η_{LL} (which was from Kaplan's
 162 equation $\tau_{LL} = \tau_{0,LL} + \eta_{LL}V$ (Kaplan 2001)), the slope of shear stress and velocity can be
 163 used to describe the property of the lubrication layer. According to Kaplan's model, the larger
 164 the viscous constant, the larger the pressure loss. Feys et al. (2014) also found that the viscous
 165 constant of the concrete mixture without fly ash was larger because of the lower thickness
 166 and higher viscosity of the lubrication layer. The viscous constant of the lubrication layer is
 167 decreased with decreasing the fine sand content and the increase of the paste volume and
 168 water-cement ratio (Feys et al. 2016). A higher content of fine sand corresponds a higher
 169 specific surface. A larger volume of paste is then needed to wrap and the viscosity is increased
 170 subsequently. The paste volume is generally considered important in the formation of
 171 lubrication layer, and it governs the amount of cement paste migrating to the lubrication layer.
 172 The increase of water-cement ratio results in the paste viscosity to decrease.

173 A correlation between the viscous constant of lubrication layer and the plastic viscosity
 174 of concrete has been found, which is affected by a number of factors. There is a complex
 175 dynamic equilibrium between the shear and the formation of the lubrication layer. The
 176 rheological properties of concrete will affect the formation, thickness and properties of the
 177 lubrication layer. The quantitative relationship between rheological parameters of the
 178 lubrication layer and pumpability of the concrete is not clear yet, and more research is well
 179 worth carrying out.

180 **4. Pumping pressure loss estimation models of pumping concrete**

181 **4.1. Conventional theoretical models**

182 Concrete is a kind of highly concentrated suspension. A few models including
 183 Bernoulli's principle, Poiseuille's law and Buckingham-Reiner's equation have been used to
 184 calculate the pumping pressure loss (Feys et al. 2014b, Secrieru 2018c). These models are
 185 given in Table 1. Based on energy conservation, Bernoulli's principle describes the pumping
 186 process of concrete from one point to another. But the ΔF , defined as the energy dissipation
 187 due to friction, is difficult to be determined. Both Poiseuille's law and Buckingham-Reiner's
 188 equation are inappropriate to describe the flow rate of pumped concrete because Poiseuille's
 189 law is valid only for incompressible Newtonian fluid with a steady laminar flow.
 190 Buckingham-Reiner's equation can significantly overestimate the experimental pressure. The
 191 pressure loss determined from Buckingham-Reiner's equation can be more than 3.8 times
 192 than the actual condition (Le et al. 2015).

193 Table 1. Theoretical models for calculations of the pumping pressure loss.

Name	Theoretical models	Requirement
Bernoulli's principle	$h_1 + \frac{p_1}{\rho g} + \frac{v_1^2}{2g} = h_2 + \frac{p_2}{\rho g} + \frac{v_2^2}{2g} + \Delta F$	Incompressible fluid, steady flow
Poiseuille's law	$Q = \frac{\pi r^4 \Delta p}{8 \eta L}$	Newtonian fluid
Buckingham-Reiner's equation	$Q = \frac{3R^4 \Delta p^4 + 16\tau_0^4 L^4 - 8\tau_0 L R^3 \Delta p^3}{24 \Delta p^3 L \mu_p}$	Bingham fluid

194
 195 Morigana's empirical formula, as shown in Eq. (8), is recommended by the Architecture
 196 Institute of Japan to calculate the pressure loss of CVC during the pumping progress (JGJ/T

197 20-2011, 2011). But the rheological properties of SCC and HFC are different from those of
 198 CVC, and the actual pumping pressure loss is much larger than that obtained from the formula
 199 (Eq. (8)). Morigana's empirical formula results in the pumping pressure loss to be around 1/5
 200 of the actual value (Li et al. 2016; Farris 1968). It is obvious that the empirical formula is not
 201 suitable for calculating the pumping pressure loss of SCC and HFC.

$$\Delta P = \frac{2a}{r} \left[K_1 + K_2 \left(1 + \frac{t_2}{t_1} \right) v \right] \quad (8)$$

202 where ΔP is the pressure loss per unit of length of the pipeline (Pa / m), a is the radial-
 203 axial pressure ratio, r is the pipeline radius (m), K_1 and K_2 are the coefficients, t_2/t_1 is
 204 the ratio of valve's switching time and piston's push time, and v is the concrete velocity
 205 (m / s).

206 4.2. Kaplan model

207 Previously reported theoretical models usually considered the influence of lubrication
 208 layer and block zone on the pumping pressure, but that the shear zone was neglected. These
 209 models are therefore not suitable for SCC and HFC with low yield stress. An important
 210 mathematical model for describing the pressure loss was proposed by Kaplan based on the
 211 pumping state with or without the shear zone of concrete in straight pipe (Kaplan 2001). The
 212 size of the wall shear stress is taken into account in Eq. (9). When the wall shear stress is less
 213 than the yield stress, Eq. (10) can be used to calculate the pressure loss in the concrete flow.
 214 Eq. (11) can be used to calculate the pressure loss when the wall shear stress is larger than
 215 the yield stress of the concrete.

$$\tau_w = \frac{\Delta p_{tot}}{L} \cdot \frac{R}{2} = \Delta p \cdot \frac{R}{2} \quad (9)$$

$$\Delta p_{tot} = \frac{2L}{R} \left(\frac{Q}{3600\pi R^2 k_r} \eta_{LL} + \tau_{0,LL} \right) \quad (10)$$

$$\Delta p_{tot} = \frac{2L}{R} \left(\frac{\frac{Q}{3600\pi R^2 k_r} - \frac{R}{4\mu_p} \tau_{0,LL} + \frac{R}{3\mu_p} \tau_0}{1 + \frac{R}{4\mu_p} \eta_{LL}} \eta_{LL} + \tau_{0,LL} \right) \quad (11)$$

216 where τ_w is the wall shear stress (Pa), Δp_{tot} is the pressure loss over the entire pipeline
 217 length (Pa), Δp is the pressure loss per unit of length of the pipeline (Pa / m), L and R are
 218 the pipeline length and the pipeline radius, respectively (m), Q is the flow rate (m^3 / h), k_r
 219 is the filling coefficient, η_{LL} is the viscous constant of lubrication layer (Pa · s / m), $\tau_{0,LL}$
 220 is the yield stress of concrete (Pa), and μ_p is the plastic viscosity of concrete (Pa · s).

221 According to above equations, the calculation of pumping pressure needs not only the
 222 rheological parameters of concrete but also the rheological parameters of the lubricating
 223 layer. Kaplan's model can be well applied for CVC, HFC and SCC (ACI 304.2R-96, 1996).
 224 However, there are still some problems to be solved when applying Kaplan's model. Firstly,
 225 the Bingham model, as adopted by Kaplan to describe the rheological behavior of fresh
 226 concrete, has been proved to have large deviations when describing the fresh concrete with
 227 shear thinning and shear thickening, but that many HFC and SCC have the rheological
 228 behavior of shear thinning or shear thickening. Secondly, the Kaplan model does not consider
 229 the influence of aggregate migration induced by shear stress on the pumping pressure loss,
 230 so it cannot well describe the performance of shear zone and block zone.

231 5. Test methods of concrete pumpability

232 **5.1. Conventional methods**

233 Slump or slump flow test is generally used to test the pumpability of fresh concrete. An
234 increase of slump normally reduces the pump pressure and improves the pumpability (Feys
235 et al. 2014). The relationship between pumping slump and pumping height is shown in Table
236 2. The ACI 304.2R-96 (1996) suggests that the slump from 50 mm to 150 mm is the most
237 suitable for pumping. This method, however, cannot simulate the key parameters for the
238 actual pumping process, for instance, the pump pipe lengths. More importantly, the crucial
239 mixture proportion parameters such as aggregate shape, grading and paste volume cannot be
240 taken into consideration while testing the pumpability of concrete (Farris 1968). In view of
241 the rheology, slump or slump flow test can only represent the yield stress of fresh concrete,
242 but not the plastic viscosity. In other words, the method recommended in ACI 304.2R-96
243 cannot fully account for the flow state of fresh concrete, and it is not suitable for modern
244 concrete with complex components.

245 The rate of pressure bleeding, an important index during the process of pumping, can be
246 used to estimate the risk of blockage. Browne et al. (1977) considered that the volume
247 difference of the pressure bleeding at 140s and 10s, noted as $\Delta = V_{140} - V_{10}$, could to some
248 extent characterize the concrete pumpability. A larger value means a higher content of
249 effective water for lubrication and a better pumpability. The relative rate of pressure bleeding
250 should not be greater than 40% at 10s according to JGJ/T 20-2011 (2011). It should be
251 pointed out that the test of pressure bleeding can only be used to judge the excess water
252 volume and the risk of plugging of the mixture for improving the mix proportion design, but
253 it cannot be used to judge the pressure loss during the pump process.

254 Table 2. Relationship between slump and pumping height (JGJ/T 20-2011, 2011).

Maximum pumping height (m)	50	100	200	400	> 400
Slump (mm)	100~140	150~180	190~220	230~260	-
Slump flow (mm)	-	-	-	450~590	600~740

255

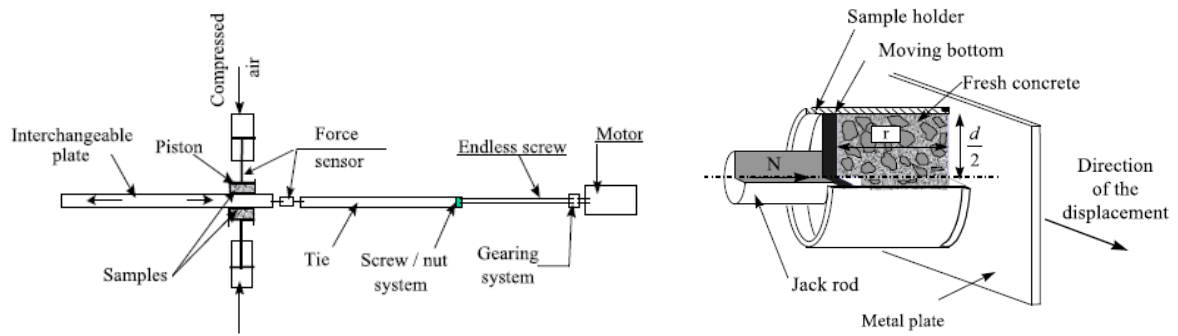
256 **5.2. Pumping circuit**

257 Testing the properties of pumped concrete by simulating flow state of concrete in the
258 rotary circular pipe has been widely recognized (Kaplan et al. 2005a). The condition of
259 pumping engineering is simulated and the results can be used to guide the construction
260 engineering directly. Whereas, the related device is not suitable to be installed in laboratory
261 because of its huge volume and complicated operation. For application of this method,
262 considerable labor force, financial resources and material resources are required.

263 **5.3. Tribometers**

264 (1) Rectilinear motion tribometer

265 The principle of the rectilinear motion tribometer is that the concrete is pressed by the
266 steel plate which slides on the surface of the compressed concrete, and the friction test is
267 carried out by the sliding steel plate and the concrete sample, as illustrated in Fig. 4. The
268 rectilinear motion tribometer can directly test the friction during the process of sliding by the
269 sensor. The properties of the interface layer are obtained accordingly. The influencing factors
270 such as roughness, sliding speed and demolding oil can be analyzed. The sealing of the test
271 process is of primary concern. Truthfully simulating the flow rate of concrete is rather
272 difficult.



273 **Figure 4.** Principle of tribometer and details of sample holder (Vanhove et al. 2004).

274 (2) Coaxial cylinder tribometer

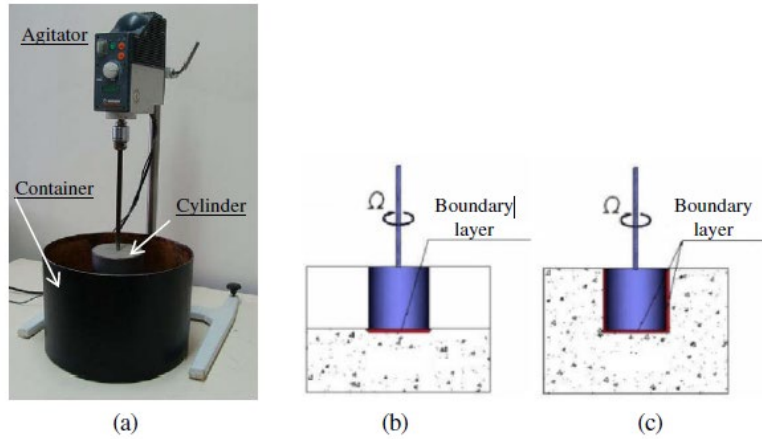
275 In order to overcome the inherent problems in rectilinear motion tribometer, Kaplan
 276 (2001) invented the coaxial cylinder tribometer (Fig. 5). The coaxial cylinder tribometer was
 277 very similar to the rheometer, and the rotation axis was not the blade but a smooth cylinder.
 278 The torques were measured at different rates to obtain the rheological parameters of the
 279 lubrication layer after the steel concrete interface was produced. It was found that the
 280 pumping data from the coaxial cylinder tribometer agreed well with the real condition. The
 281 results obtained can be used to well describe the properties of the lubrication layer, but that
 282 a high sensibility of the coaxial cylinder tribometer to test the yield stress of lubrication layer
 283 has been found. Repeated measurements are required to obtain accurate results.

284 Part of the tribometer is sealed and the additional friction is unavoidable in the rotation
 285 test process. Hence Ngo et al. (2010a, 2010b) developed another kind of coaxial cylindrical
 286 tribometer, as shown in Fig. 6. In addition, Feys et al. (2015) stated that the coaxial cylinder
 287 tribometers developed by previous scholars were used mainly to test the CVC and were not
 288 suitable for HFC and SCC with low yield stress. As such, Feys et al. (2014) developed a new
 289 kind of coaxial cylinder tribometer (Fig. 7), by which the properties of lubrication layer of
 290 HFC and SCC can be characterized by appropriate measurement procedures and data
 291 processing. It is worthwhile to note that there may be deviation during the measurement of
 292 the coaxial cylinder tribometer, because of the dynamic segregation of concrete that results
 293 from blades turning (Yan 2018).



294
 295

Figure 5. Coaxial cylinder tribometer developed from Kaplan (2001).



296
297

Figure 6. Coaxial cylinder tribometer developed from Ngo et al. (2010a, 2010b).

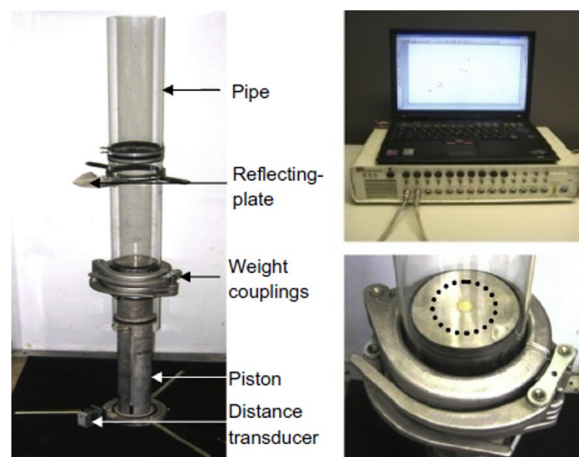


298
299

Figure 7. Coaxial cylinder tribometer developed from Feys et al. (2014).

300 (3) Sliding pipe rheometer

301 Sliding pipe rheometer, as displayed in Fig. 8 (Kasten 2009), enables to simulate
 302 concrete pumping and readily obtains pumping parameters. The lubrication layer in sliding
 303 pipe is formed while concrete sliding in the pipe. The sliding pipe rheometer is equipped with
 304 different falling weight, and the pressure and sliding speed of the top piston are tested
 305 simultaneously. The relationship between the pressure and the flow rate is obtained by the
 306 data processing after measurements.



307
308

Figure 8. Sliding pipe rheometer and its components (Yan 2018).

309 Sliding pipe rheometer is convenient. The rheological parameters of low slump concrete
 310 can be tested by the sliding pipe rheometer, as opposed to the coaxial cylinder tribometer.

311 The test results are in good agreement with the experimental data (Zhao 2014). However, the
312 sliding pipe rheometer only considers the friction zone, with the shear zone not considered,
313 and it cannot reflect the real pumping velocity due to limitations of the device. The fact that
314 sliding pipe rheometer is in general an effective tool to study the properties of pumped
315 concrete makes it suitable for studying the pumping properties in the laboratory.

316 **6. Factors influencing the concrete pumpability**

317 The pumpability of concrete has been studied since the last century. The pumpability of
318 concrete is influenced by a range of factors (Djelala et al. 2004). Using a single parameter to
319 represent the concrete pumpability is certainly not reliable. This section reviews the
320 influencing factors of concrete pumpability from four different aspects including the
321 composition, rheological parameters, workability, and the external factors.

322 **6.1. Concrete composition**

323 (1) Raw materials

324 Concrete pumping depends on the properties of the concrete in the pipe. Mechtcherine
325 et al. (2014) analyzed changes of pumping performance by pump pressure-flow curves for
326 different concrete mixtures. The results indicated that in case other factors are the same, using
327 granular aggregate has a higher pumpability than using crushed aggregate. The crushed
328 aggregate has a larger specific surface area than the granular aggregate. Therefore, the
329 crushed aggregate needs more pastes to enwrap during pumping (Ragan 1981; Bouquety et
330 al. 2007). In addition, the flowability of the mixture is worse because of the interlocked effect
331 of the crushed aggregates (Aissoun et al. 2015; Fung et al. 2013). An increase of the aggregate
332 volume-fraction by around 10% results in a decrease of the concrete pumpability by at least
333 30% (Fataei et al. 2020). This finding is particularly pronounced for CVC (Fataei et al. 2019).
334 Blockage can take place due to arch formation of the roughest particles. A higher content of
335 coarse aggregate particles will increase the risk of blocking of the pipe. Hardened blocked
336 concrete in pipes has been reported, among others, by Kaplan et al. (2005a). The blocking
337 mechanism can be ascribed to forward segregation, owing to acceleration of large particles
338 during the stroke of piston pumps (Jacobsen et al. 2009). Bend pipes have a higher risk of
339 blocking than tapered ones. A severe segregation of mixture components should be avoided
340 in order to prevent blockage (Mechtcherine et al. 2014). Adding silica fume with appropriate
341 content enables to obtain a better pumpability than adding fly ash (Vanhove et al. 2004). The
342 mixture with fly ash has lower viscous constant and viscosity than the mixture without fly
343 ash (Djelala et al. 2004).

344 (2) Mix proportion

345 Zhao (2014) analyzed the effects of factors, including water-cement ratio, paste volume,
346 air content, coarse aggregate and mineral admixture, on the pumping performance of
347 concrete. The results showed that for CVC in the appropriate range, increasing paste volume,
348 entraining air, and using larger size of aggregate were favorable to reduce the pumping
349 resistance and thus improving the pumpability (Best et al. 1980). Supplementary
350 cementitious materials such as fly ash and granulated blast furnace slag have been reported
351 to increase the flowability due to the densified particle packing density and the ball bearing
352 effect of particles (Ferraris et al. 2001). The silica fume, normally very fine in particle size,
353 will affect the flowability and pumping behavior of fresh concrete. The yield stress of
354 cement-based materials is normally decreased when incorporating ultra-fine admixtures. The
355 viscosity, however, varying significantly with different types of admixtures, decreases with
356 the addition of ultra-fine slag, fly ash and silica fume, but increases by adding anhydrous

357 gypsum. Superplasticizer plays an important role, and its dosage is almost linearly correlated
358 with the pumping performance, as reported by Jeong et al. (2016).

359 The concrete pumpability can be enhanced by increasing the cement paste volume,
360 water-cement ratio and superplasticizer dosage (Ling et al. 2015; Ngo et al. 2012). Although
361 the increase of the water-cement ratio can improve pumpability, it is easy to induce
362 segregation, bleeding and pipe blockage in the pumping process (Mai et al. 2014; Felekoglu
363 et al. 2007). The pumpability is highly associated with both the workability and stability of
364 the fresh concrete. Based on the principle of balancing effect, Anderson (1977) suggested ten
365 relevant guidance that can be used to analyze raw materials and mix proportion for
366 preparations of pumping concrete with good pumpability.

367 **6.2. Rheological parameters**

368 The rheological behavior of concrete can be described using the pressure loss-flow
369 relationship. A good correlation between the two exists for self-compacting concrete. For
370 normal concrete the yield stress is a dominant factor. The rheological parameters can be
371 influenced after changes of the concrete composition (Siddique et al. 2012), and the
372 pumpability is affected accordingly. Zerbino et al. (2009) established a relationship between
373 rheological parameters and pressure loss based on studies of fresh concrete with different
374 mix proportions. The yield stress and plastic viscosity of all concretes were measured. They
375 found a good correlation between the plastic viscosity and the pressure loss, regardless of the
376 type of concrete. For yield stress, a clear relationship could only be observed for CVC, but
377 not for SCC and HFC. This can be ascribed to the fact that the yield stress-to-plastic viscosity
378 ratio is the dominant factor for shearing flow. The yield stress becomes increasingly
379 important at lower viscosity. Different values of rheological parameters may be acquired for
380 the same mixtures when testing by different instruments (Mai et al. 2014).

381 Kaplan et al. (2005b) reported that the viscous constant (rather than the yield stress) of
382 the lubrication layer was the major factor for pumpability. Differently from other workers
383 (Felekoglu et al. 2007), Feys et al. (2014) measured the values of viscous constant of
384 lubrication layers and found a good relationship between the measured pressure loss and the
385 viscous constant. Unfortunately, it is not clear whether the observed relationship results from
386 the viscous constant of the lubrication layer or the plastic viscosity of the bulk concrete. From
387 Kaplan's model, the rheological parameters of concrete play important roles in the pumping
388 pressure loss. The change of rheological parameters will lead to the change of pumpability
389 (Ngo et al. 2011).

390 **6.3. Workability**

391 It is difficult to measure the pumpability in laboratory by the full-scale simulation of
392 pumping owing to the large space required and the high cost. On the other hand, the
393 pumpability can be investigated according to the performances of multiple sections that can
394 be tested and evaluated separately. As stated earlier, the slump and rate of pressure bleeding
395 have been used to estimate the pumpability in a few codes. Entraining air (about 3-5%) has
396 advantages in preventing bleeding and improving the workability. A high entraining air
397 content, however, results in the compressibility to be increased, leading to unstable pumping
398 pressure (Aissoun et al. 2015).

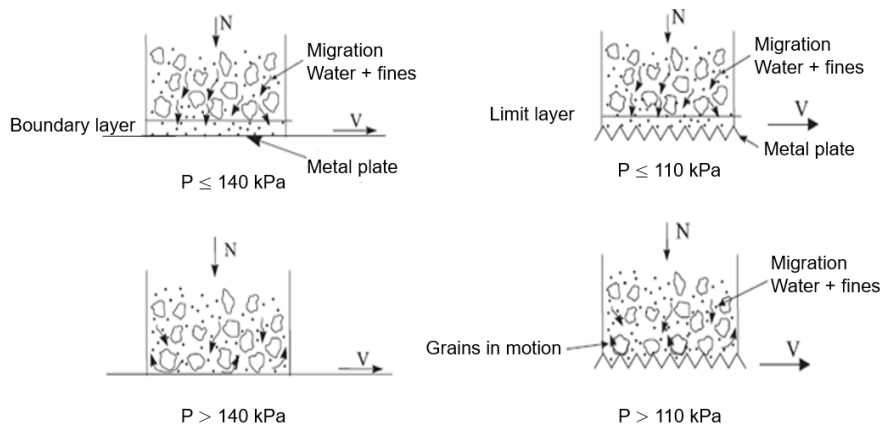
399 There is a very good correlation between the pump pressure loss and the V-funnel flow
400 time of SCC (Yun et al. 2015). The pressure loss of SCC with low yield stress is affected
401 mainly by the plastic viscosity, and there may be a direct correlation between the V-funnel
402 flow time and the plastic viscosity of concrete mixture.

403 The traditional tests are easy to operate and can rapidly figure out the workability in a
404 qualitative manner, and are therefore suitable to be used in the construction site (Laskar
405 2009). It is meaningful to establish a relationship between the traditional tests and the
406 rheological parameters in order for guiding the pumping construction in practical projects.

407 **6.4. External factors**

408 Apart from the concrete itself, other external factors such as the diameter of pump pipe
409 and the equivalent length of bent pipe can also affect the concrete pumpability. By
410 establishing 148m test pipeline to simulate the full-scale pumping process, Kaplan (2001)
411 found that the poor design of pumping pipeline system and the inappropriate operation would
412 induce blockage. It is appropriate to pump at low speed at the beginning for lubricating the
413 pipe. The diameter of the pipe should be 4 times larger than the maximum size of the
414 aggregate used in the mixture. Otherwise the air would easily get into the pipe forming gas
415 bubbles disrupting the stable flow state of fresh mixture. The bent pipe increases the
416 additional pressure loss for SCC but not for CVC (Kaplan et al. 2005b), and the real pressure
417 loss is higher than the value calculated from the rule of thumb. By studying the flow behavior
418 of two pipes with varying diameters, Feys et al. (2016) found that the pressure loss was
419 increased by a factor of 2 for a 20% reduction in the pipe diameter.

420 Vanhove et al. (2008) studied the friction behavior between SCC and steel plate with
421 different roughness. A summary of the friction mechanism is shown in Fig. 9. As indicated,
422 there are different critical pressures in the sliding process. According to Kaplan's model, the
423 flow velocity, the diameter and the pipe length all affect the required pumping pressure and
424 pumpability. In principle more energy is required in case of an increase of pumping height.



425

426

Figure 9. Friction mechanism of different steel plates and pressures.

427 **7. Typical constructions of ultra-high pumped concrete in China**

428 There is a growing demand globally for large-scale constructions, such as long-span
429 bridges, high-rise buildings, long-distance tunnels, etc., which has triggered the large-scale
430 pumping research all over the world (Choi et al. 2014, De Schutter 2017, Secrieru et al.
431 2018a, Secrieru et al. 2020). Knowledge of the pumping flow rate and rheological properties,
432 particularly yield stress and plastic viscosity, is often required. Related parameters, including
433 concrete composition, strength grade, pumping height, etc., are of paramount importance in
434 the large-scale concrete pumping. Numerical simulation and experimental verification were
435 intensively combined to characterize and predict the concrete pumping behavior. Chio et al.
436 (2013) applied the Computational Fluid Dynamics (CFD) approach to study the properties of
437 the lubrication layer. The influence of the yield stress on the lubrication layer was neglected.
438 The concrete velocity profile and rheological properties were measured by means of
439 Ultrasonic Velocity Profiler and Brookfield DV-II viscometer, respectively. An analytical
440 relation was proposed that can be roughly estimate the pumping pressure. Secrieru et al.
441 (2020) simulated the flow pattern using the CFD approach. The semi implicit method
442 implemented for pressure linked equations was applied for the pressure-velocity coupling.
443 The concrete flow behavior was simulated by the single-fluid approach. It was found that the

444 simulated results were in good agreement with those derived from full-scale rheological tests
 445 before and after pumping.

446 In recent decade large-scale constructions, as well as large-scale concrete pumping
 447 practice, have taken place more rapidly in China than other countries. In China a large
 448 number of ultra-high buildings above 300m have been built or are being built, which have
 449 greatly promoted the advancement of the theory and technology of large-scale concrete
 450 pumping. Over the recent decade the technology of high strength, high flow and low viscosity
 451 self-compacting concrete has developed rapidly. This section provides six typical ultra-high
 452 pumping construction projects in China as examples to introduce the development of high
 453 strength self-compacting concrete ultra-high pumping construction technology in China. The
 454 details of these engineering examples are shown in Table 3 and Table 4 (Chen et al. 2016;
 455 Gu 2009; Li et al. 2016; Ran et al. 2011; Yu et al. 2011; Zhang et al. 2017).
 456

457 Table 3. Examples of ultra-high pumped concrete engineering in China.

Name	Structural height (m)	Layer number	Floor area (m ²)	Maximum strength grade of concrete	Pumping height (m)
International Finance Centre	420	88	200000	C90	392
KingKey Financial Center	442	98	602402	C120	422
Guangzhou International Finance Centre	440	103	450000	C90/C60	168/432
Tianjin 117 building	597	117	1960000	C60	621
Shanghai World Financial Center	492	101	381600	C60	492
CITIC Tower	528	108	437000	C70	528

458

459 Table 4. Concrete proportioning of the ultra-high pumped concrete engineering
 460 (kg/m³).

Name	Portland cement	Fly ash	Silica fume	Sand	Gravel	Water	Water reducer	Slump flow (mm)
International Finance Centre	370	180	35	600	1000	152	2.9	700
KingKey Financial Center	500	170	80	700	1000	130	26.0	650
Guangzhou International Finance Centre	430	145	40	729	1000	130	16.0	600
Tianjin 117 building	297	143	33	850	850	160	8.8	650
Shanghai World Financial Center	440	110		800	870	175	7.2	650
CITIC Tower	360	180	40	760	850	160	6.6	700

461

462 The first Guinness World Records concerning Chinese concrete industry was created by
463 the construction engineering of Tianjin 117, and the high-performance concrete with C60
464 was pumped to the height of 621m (Ngo et al. 2011). The experimental database used for
465 simulating the ultra-high pumping was established, which aimed to solve the technical
466 problems in real engineering. The superplasticizer developed in China has contributed
467 significantly to solving the problems of large loss of workability, high viscosity in high
468 strength concrete, dispersing easily in low strength concrete, and so on.

469 **8. Conclusions**

- 470 1) The flow state of pumped concrete in horizontal pipe comprises friction flow and viscous
471 flow. CVC moves mainly by friction flow in the pipe, while SCC and HFC move
472 concurrently by friction flow and viscous flow due to the low yield stress.
- 473 2) Viscous flow includes three parts: lubrication layer, block zone and shear zone.
474 Lubrication layer, consisting of water, cementitious materials, and fine sand with
475 diameter smaller than 0.25 mm, plays a dominant role in the pumping process. It is
476 meaningful in practice to characterize the pumpability by measuring the properties of
477 lubrication layer. The shear zone has a great influence on the pumping performance of
478 the fresh concrete, but that the studies regarding the influencing mechanism of shear
479 zone on the fresh concrete pumpability are far from sufficient.
- 480 3) It is not reliable for the conventional theories and models to describe the pumping of
481 modern concrete, e.g. SCC and HFC. The particle diffusive models, in combination with
482 special rheological model, can be used only to predict the flow rate. Kaplan's model is
483 applicable for CVC and SCC, but it cannot explain the changes in the air content and
484 slump/slump flow of the fresh concrete before and after pumping.
- 485 4) Simulation experiment is considered a comprehensive, effective and direct method to
486 evaluate the concrete pumpability. Coaxial cylinder tribometer and slipper can quantify
487 the pumpability and can be used in field tests.
- 488 5) The pumpability of modern concrete is affected by concrete composition, workability,
489 thixotropy, pressure, shear behavior, temperature and other factors. Understanding the
490 tribology of lubrication layer, along with the effects of these factors on the concrete
491 rheology, is helpful to capture the pumping mechanism of modern concrete.

492 **Acknowledgments**

493 This research was funded by the National Key R&D Plan of China (Grant No.
494 2017YFB0310100), the National Natural Science Foundation of China (Grant No.
495 U1934206, 51578545) and the Technological Research and Development Programs of China
496 Railways Corporation (No. 2017G006-J, N2018G029 and J2017G001).

497 **Conflicts of Interest**

498 The authors declare no conflict of interest.

499 **References**

- 500 ACI 304.2R-96. (1996). "Placing concrete by pumping methods."
501 Aissoun, B.M., Hwang, S.D. and Khayat, K.H. (2015). "Influence of aggregate
502 characteristics on workability of superflowability concrete." *Materials and Structures*,
503 49, 1-13.

504 Andreson, W.G. (1977). "Analyzing concrete mixtures for pumpability." *Journal of the*
505 *American Concrete Institute*, 74, 447-451.

506 Best, J.F. and Lane, R.O. (1980). "Testing for optimum pumpability of concrete." *American*
507 *Society of Civil Engineers*, pp. 49-61.

508 Bouquety, M.N., Descantes, Y., Barcelo, L., Larrard, F.D. and Clavaud, B. (2007).
509 "Experimental study of crushed aggregate shape." *Construction and Building Materials*,
510 21, 865-872.

511 Browne, R.D. and Bamforth, P.B. (1977). "Tests to Establish Concrete Pumpability." *ACI*
512 *Structural Journal*, 74, 193-203.

513 Chen, Q., Yuan, Q., Luo, Z. and Zhao, Z. (2016). "Development and engineering application
514 of ultra-high pumping concrete in Tianjin high silver 117 building." *Construction*
515 *Technology*, 45, 16-20.

516 Choi, M.S., Roussel, N., Kim, Y.J. and Kim, J.K. (2013). "Lubrication layer properties during
517 concrete pumping." *Cement Concrete Research*, 45, 69-78.

518 Choi, M.S., Kim, Y.S., Kim, J.H., Kim, J.S. and Kwon, S.H. (2014). "Effects of an externally
519 imposed electromagnetic field on the formation of a lubrication layer in concrete
520 pumping." *Construction and Building Materials*, 61, 18-23.

521 De Schutter, G. (2017). "Thixotropic effects during large-scale concrete pump test on site."
522 International Conference on Advances in Construction Materials and Systems. Ed. Manu
523 Santhanam et al. Paris: RILEM Publications, 2, 1-7.

524 Djelala, C., Vanhove, Y. and Magnin, A. (2004). "Tribological behaviour of self-compacting
525 concrete." *Cement and Concrete Research*, 34, 821-828.

526 Ede, A.N. (1957). "The resistance of concrete pumped through pipelines." *Concrete*
527 *Research*, 9, 129-140.

528 Farris, R.J. (1968). "Prediction of the viscosity of multimodal suspensions from unimodal
529 viscosity data." *Journal of Rheology*, 12 (2), 281-301.

530 Fataei, S., Secrieru, E., and Mechtcherine, V. (2019). "Influence of aggregate volume fraction
531 on concrete pumping behaviour. *Rheology and Processing of Construction Materials*,
532 23, 303-310.

533 Fataei, S., Secrieru, E. and Mechtcherine, V. (2020). "Experimental Insights into Concrete
534 Flow-Regimes Subject to Shear-Induced Particle Migration (SIPM) during Pumping."
535 *Materials*, 13, 1233.

536 Felekoglu, B., Turkel, S. and Baradan, B. (2007). "Effect of water/cement ratio on the fresh
537 and hardened properties of self-compacting concrete." *Building and Environment*, 42,
538 1795-1802.

539 Ferraris, C.F., Obla, K.H. and Hill, R. (2001). "The influence of mineral admixtures on the
540 rheology of cement paste and concrete." *Cement and Concrete Research*, 31 (2), 245-
541 255.

542 Feys, D., Khayat, K.H. and Khatib, R. (2016). "How do concrete rheology, tribology, flow
543 rate and pipe radius influence pumping pressure?" *Cement and Concrete Composites*,
544 66, 38-46.

545 Feys, D., Khayat, K.H., Perez-Schell, A. and Khatib, R. (2014). "Development of a
546 tribometer to characterize lubrication layer properties of highly-workability concrete."
547 *Cement and Concrete Composites*, 54, 40-52.

548 Feys, D., Khayat, K.H., Perez-Schell, A. and Khatib, R. (2015). "Prediction of pumping
549 pressure by means of new tribometer for high-flowability concrete." *Cement and*
550 *Concrete Composites*, 57, 102-115.

551 Feys, D., Verhoeven, R. and Schutter, G.D. (2009). "Pipe flow velocity profiles of complex
552 suspensions, like concrete." *National Congress of Theoretical and Applied Mechanics*,
553 pp. 66-73.

554 Fung, W.W.S. and Kwan, A.K.H. (2013). "Effect of particle interlock on flow of aggregate
555 through opening." *Powder Technology*, 253, 198-206.

556 Gu, G. (2009). "Preparation, production and ultra high pumping technology of C100 and
557 C100 self compacting concrete for Guangzhou West Tower Project." *Science and
558 Technology*, 7, 31-41.

559 Jacobsen, S., Haugan, L., Hamme, T.A. and Kalogiannidis, E. (2009). "Flow conditions of
560 fresh mortar and concrete in different pipes." *Cement Concrete Research*, 39, 997-1006.

561 Jeong, J.H., Jang, K.P., Park, C.K., Lee, S.H. and Kwon, S.H. (2016). "Effect of admixtures
562 on pump ability for high-strength concrete." *ACI Materials Journal*, 113 (3), 323-333.

563 JGJ/T 20-2011. (2011). "Technical specification for construction of concrete pumping." (In
564 Chinese).

565 Jiang, Z., Tao, Z. and Ren, Q. (2017). "Study on pump pressure law of self compacting
566 concrete with mechanical sand." *Journal of Building Materials*, 20, 18-23.

567 Jo, S.D., Chan, K.P., Jeong, J.H., Lee, S.H. and Kwon, S.H. (2012). "A computational
568 approach to estimating a lubricating layer in concrete pumping." *CMC-Computer
569 Materials Continua*, 27 (3), 189-210.

570 Jolin, M., Burns, D., Bolduc, L.S, Bissonnette, B. and Gagnon, F. (2009). "Understanding
571 the pumpability of concrete." In: Shotcrete for underground support XI – engineering
572 conferences international, proceeding.

573 Kaplan, D. (2001). "Pumping of Concretes." Ph.D-thesis (in French), Laboratoire Central des
574 Ponts et Chaussees, Paris.

575 Kaplan, D., De Larrard, F. and Sedran, T. (2005a). "Avoidance of blockages in concrete
576 pumping process." *ACI Materials Journal*, 102, 183-191.

577 Kaplan, D., De Larrard, F. and Sedran, T. (2005b). "Design of concrete pumping circuit."'
578 *ACI Materials Journal*, 102 (2), 110-117.

579 Kasten, K. (2009). "Gleitrohr Rheometer, Ein Verfahren zur Bestimmung der
580 Fließeigenschaften von Dickstoffen in Rohrleitungen (in German)." Ph.D-thesis,
581 Technische Universität Dresden.

582 Kwon, S.H., Chan, K.P., Jeon, J.H., Jo, S.D. and Lee, S.H. (2013). "Prediction of concrete
583 pumping: Part I-development of new tribometer for analysis of lubricating layer." *ACI
584 Materials Journal*, 110 (6), 647-655.

585 Laskar, A. and Talukdar, S. (2009). "Rheology-based approach for workability
586 characterization of high-performance concrete." *Canadian Journal of Civil Engineering*,
587 36, 1239-1244.

588 Le, H.D., Kadr, E.H., Aggoun, S. and Vierendeels, J. (2015). "Effect of lubrication layer on
589 velocity profile of concrete in a pumping pipe." *Materials and Structures*, 48, 1-13.

590 Li, L., Chen, X., Zhang, L. and Li, L. (2016). "Discussion on construction technology of
591 concrete pumping for super high-rise buildings." *Architecture Technology*, 45, 335-338.

592 Mai, C.T., Kadri, E.H., Ngo, T.T., Kaci, A. and Riche, M. (2014). "Estimation of the
593 Pumping Pressure from Concrete Composition Based on the Identified Tribological
594 Parameters." *Advanced Materials and Science and Engineering*, 503850, pp. 1-18.

595 Mechtcherine, V., Nerella, V.N. and Kasten, K. (2014). "Testing pumpability of concrete
596 using sliding pipe rheometer." *Construction and Building Materials*, 53, 312-323.

597 Morinaga, M. (1973). "Pumpability of concrete and pumping pressure in pipeline." Proc.
598 RILEM Seminar on Fresh Concrete: Important Properties and their Measurement, Leeds.
599 7, 1-39.

600 Li, L. and Chen, X. (2016). "Analysis of pumping pressure variation law of self-compacting
601 concrete." *Construction Technology*, 45, 52-56.

602 Ling, S.K. and Kwan, A.K.H. (2015). "Adding ground sand to decrease paste volume,
603 increase cohesiveness and improve passing ability of SCC." *Construction and Building
604 Materials*, 84, 46-53.

605 Ngo, T., Kadri, E., Bennacer, R. and Cussigh, F. (2011). "Measurement and modeling of
606 fresh concrete viscous constant to predict pumping pressures." *Canadian Journal of*
607 *Civil Engineering*, 38, 944-956.

608 Ngo, T., Kadri, E., Bennacer, R. and Cussigh, F. (2010a). "Use of tribometer to estimate
609 interface friction and concrete boundary layer composition during the fluid concrete
610 pumping." *Construction and Building Materials*, 24, 1253-1261.

611 Ngo, T., Kadri, E., Cussigh, F., Bennacer, R. and Duval, R. (2010b). "Practical tribometer to
612 estimate pumpability of fresh concrete." *Journal of Asian Architecture and Building*
613 *Engineering*, 9, 229-236.

614 Ngo, T., Kadri, E., Cussigh, F. and Bennacer, R. (2012). "Relationships between concrete
615 composition and boundary layer composition to optimise concrete pumpability." *European Journal of Environment and Civil Engineering*, 16, 697-708.

616 Ragan, S.A. (1981). "Valuation of tests for determining the pumpability of concrete
617 mixtures." Laboratory Tests.

618 Ran, Z., Yan, L. and Guo, Y. (2011). "Comprehensive construction technology of Shenzhen
619 Jing Ji 100". *Construction Technology*, 40, 10-14.

620 Rossig, M. and Frischbeton, F.V. (1974). "Insbesondere von Leichtbeton, durch
621 Rohrleitungen (In German)." Rheinisch-Westfälische Technische Hochschule,
622 Westdeutscher Verlag, ISBN 3-531-02456-6.

623 Secrieru, E., Cotardo, D., Mechtcherine, V., Lohaus, L., Schröfl, C. and Begemann, C.
624 (2018a). "Changes in concrete properties during pumping and formation of lubricating
625 material under pressure." *Cement and Concrete Research*, 108, 129-139.

626 Secrieru, E. (2018b). "Pumpverhalten moderner Betone - Charakterisierung und Vorhersage
627 - Pumping behaviour of modern concretes - Characterisation and prediction (in
628 German)", Ph.D.-thesis, Technische Universität Dresden.

629 Secrieru, E. Khodor, J., Schröfl, C., Mechtcherine, V. (2018c). "Formation of lubricating
630 layer and flow type during pumping of cement-based materials." *Construction and*
631 *Building Materials*, 178, 507-517.

632 Secrieru, E., Fataei, S. and Mechtcherine, V. (2020). "Assessment and prediction of concrete
633 flow and pumping pressure in pipeline." *Cement and Concrete Composites*, 107, 103495.

634 Siddique, R., Aggarwal, P. and Aggarwal, Y. (2012). "Influence of water/powder ratio on
635 strength properties of self-compacting concrete containing coal fly ash and bottom ash." *Construction and Building Materials*, 29, 73-81.

636 Vanhove, Y., Djelal, C. and Magnin, A. (2004). "A Device for Studying Fresh Concrete
637 Friction." *Cement Concrete and Aggregate*, 26, 35-41.

638 Vanhove, Y., Djela, C. and Chartier, T. J. (2008). "Ultrasonic wave reflection approach to
639 evaluation of fresh concrete friction." *Advanced Concrete Technology*, 6, 253-260.

640 Yan, P. and Li, M. (2018). "Pumpability of fresh concrete-an overview." *Journal of Chinese*
641 *ceramic Society*, 1, 2-46.

642 Yu, C. and Shi, W. (2011). "Pumping concrete technology and ultra high pumping concrete
643 technology." *Beton Chinese Edition - Ready-mixed Concrete*, 10, 29-34.

644 Yun, K.K., Choi, P., and Yeon, J.H. (2015). "Correlating rheological properties to the
645 pumpability and shootability of wet-mix shotcrete mixtures." *Construction and Building*
646 *Materials*, 98, 884-891.

647 Zerbino, R., Barragan, B., Garcia, T., Agullo, L. and Gettu, R. (2009). "Workability tests and
648 rheological parameters in self-compacting concrete." *Materials and Structures*, 42, 947-
649 960.

650 Zhang, J. and Liu, G. (2017). "Structural design of Shanghai international financial center." *Building and Structures*, 47, 48-52.

651 Zhao, J. (2014). "The research progress of evaluation method for pumpability test of pumped
652 concrete (in Chinese)." *Building Decoration Materials World*, 4, 44-53.

656 Zhao, Z. (1985). "Pumping concrete (in Chinese)." China Architecture & Building Press, 3,
657 68-112.